

# Magnetorotational Instability around a Rotating Black Hole

M. Yokosawa and T. Inui

*Department of Physics, Ibaraki University, Mito, Japan 310-8512*

## ABSTRACT

The magnetorotational instability (MRI) in the Kerr spacetime is studied on a 3+1 viewpoint. The Maxwell's equations are expressed in a circularly orbiting observer's frame that co-rotates with matter in Keplerian orbits. The hydromagnetic equations are represented in a locally nonrotating frame (LNRF). There exist large proper growth rates in MRI around a rapidly rotating black hole. The large "centrifugal force" and the rapid variations of magnetic fields are caused by the rotation of spacetime geometry. As the result, in the extreme Kerr case the maximum proper growth rate at  $r = r_{ms}$  becomes about twelve times as large as that in Schwarzschild case, where  $r_{ms}$  is the radius of a marginally stable orbit. The unstable range of wavenumber expands according to the rotational speed of spacetime geometry. The over stable mode of the instability becomes remarkable when the circular motion of the disk is quasi-relativistic and the strength of magnetic field is so large that the Alfvén velocity is  $v_A \geq 0.1c$ . When the waves of perturbations propagate in the radial direction, these waves oscillate and their amplitudes grow exponentially. This instability is caused by the differential rotation of the circularly orbiting frame. The universality of the local Oort  $A$ -value of the disk is discussed in curved spacetime. In the extreme Kerr geometry, the amplitude of the maximum growth rate in the dynamical shear instability (DSI) reaches to infinity at  $r = r_{ms}$ . The behaviors of maximum growth rates between MRI and DSI are remarkably different each other.

*Subject headings:* accretion — hydromagnetics: instabilities — turbulence: relativity — black hole

## 1. Introduction

The various intensive phenomena, x-ray or  $\gamma$ -ray emission, jet, etc. are found in many active objects. Some intense  $\gamma$ -ray bursts (GRBs) are believed to arise from the hot, dense matter accretion onto a rotating black hole (Popham, Woosley & Fryer 1999; Di Matteo,

Perna, & Narayan 2002; Kohri, & Mineshige 2002; Yokosawa, Uematsu & Abe 2004). The viscosity is the important physical quantity to balance the heat in the disk and to determine the dynamics of the accretion. The magnetohydrodynamical turbulent viscosity is driven by the magnetorotational instability (MRI) (Balbus & Hawley 1991; Hawley & Balbus 1991; Hawley, Gammie, & Balbus 1995; Brandenburg et al. 1995; Matsumoto & Tajima 1995; Stone et al. 1996; Balbus & Hawley 1998). We study here the MRI on the basis of the general relativistic magnetohydrodynamics.

The MRI in the Kerr metric had been considered by Gammie (2004). He had analyzed the dynamical shear instability(DSI) for circularly orbiting particles. The maximum growth rate in MRI was then discussed according to the analogy between DSI and MRI. It had been previously shown by Balbus & Hawley (1992) that in a Newtonian case the both maximum growth rates in MRI and DSI coincide each other. However its consistency is not always satisfied in general spacetime. The MRI in curved spacetime should be investigated on the general relativistic Maxwell's equations and hydrodynamics, and then be examined for the consistency of the maximum growth rate between the two types of instabilities.

The generation of MRI is caused by the two processes; the strengthen of magnetic field due to the differential rotations of the disk, and the transfer of angular momentum by magnetic stress (Balbus & Hawley 1998). The rotation of the spacetime geometry exerts the characteristic effects on the kinematics and on the induction of magnetic field. In the rotating spacetime geometry, there appears "the gravitomagnetic force" which is an inertial force in 3+1 point of view (Thorne et al. 1986; Punsly 2001). The gravitomagnetic force depends on the gradient of the geometrical angular velocity,  $\nabla\omega$ . The gravitomagnetic force exerts a torque on a spin outside a black hole (Thorne et al. 1986) and strengthens the centrifugal force. The increased radial velocity then induces the large variation of magnetic fields which transfer the angular momentum. The rotating velocity of the disk becomes extremely large in the vicinity of a rapidly rotating black hole. The changing rate of magnetic field due to the differential rotation of the disk is then largely increased. The generation of MRI may be very active around a rapidly rotating black hole.

It is useful to introduce the 3+1 formulation of general relativity which is excellent to make clear the physics on the stability. The evolutions of the perturbations are then simply evaluated by the analogous terms to the Newtonian dynamics and to the Maxwell equations in flat spacetime. We introduce the Keplerian orbiting observer's frame (orbiting frame) to evaluate the electromagnetic fields perturbed by the motion of fluid. On the other hand the dynamic equations of fluid interacting with magnetic fields are analyzed in the locally non-rotating frame(LNRF)(Bardeen et al. 1972) since this frame becomes an inertial frame at the far distance from a black hole. Thus the dispersion relation expressed in these frames

approaches to a Newtonian one at the far distance.

When the Maxwell equations are described in the orbiting frame, there appear explicitly the electromagnetic fields generated by the frame moving . When the rotating velocity of the frame is relativistic, the induction of magnetic field by the differential rotation of the orbiting frame becomes efficient. This generation of magnetic field causes an overstable mode of instability. We investigate here the characteristic behaviors of this new mode in MRI.

The intensive phenomena in active objects may be produced by the nonstationary magnetohydrodynamical processes in the accretion disk around a rotating black hole. We are interesting in the spatial distribution of a growth rate of MRI. Yokosawa, Uematsu & Abe (2004) had represented the angular velocity of circular orbits for a geometrically thick disk,  $\Omega(r, z)$ . By using this angular velocity  $\Omega(r, z)$ , we investigate the distribution of the maximum growth rate  $\Gamma_{max}(r, z)$  over the space around a rotating black hole.

When the geometry of spacetime rotates, it is important to select the suitable frame for the analysis of the instability. In the Boyer-Lindquist coordinate frame (BLCF) the dragging of inertial frames becomes so severe that the  $t$  coordinate basis vector ( $\partial/\partial t$ ) goes spacelike at the static limit  $r_0$  (outer boundary of the ergosphere). In LNRF the frame dragging effects of the hole's rotation are canceled out. Gammie (2004) investigated the DSI in BLCF. We reanalyze the upper bound to the growth rate of DSI in LNRF by using the general relativistic Hill equations. We then examine the asymptotic behaviors of the growth rates for  $r \rightarrow r_{ms}$  when the frame is exchanged from BLCF to LNRF. We inquire the suitable frame to evaluate the instability, MRI or DSI. The universality of local Oort  $A$ -value in the shear instability is then examined by comparing the dispersion relations for DSI and MRI in the suitable frame.

In the next section we shall describe the Maxwell's equations in the orbiting frame and the magnetohydrodynamic equations in LNRF. The dispersion relation and the properties of growth rates in curved spacetime are analyzed in the section 3. The universality of the growth rate of the shear instability in general, gravitational field is discussed in section 4.

## 2. Basic Equations

The preferred frame describing the basic equations is selected definitely to evaluate the perturbations. The LNRF becomes an inertial frame at the infinite distance from a black hole. Thus the characteristic frequencies in dynamics, e.g., epicyclic frequency, are definitely expressed in LNRF. The perturbations of hydrodynamics are represented in LNRF. The perturbations of magnetic field exerting on the fluid are simply evaluated in the frame co-

moving with the fluid in a Keplerian orbit (Punsly 2001). The both frames, LNRF and orbiting frame, are combined with the Lorenz transformation.

We choose units with  $G = c = 1$ . The metric of spacetime, in terms of Boyer-Lindquist time  $t$  and any arbitrary spatial coordinates  $x^j$ , has the form

$$ds^2 = -\alpha^2 dt^2 + g_{jk}(dx^j + \beta^j dt)(dx^k + \beta^k dt). \quad (1)$$

The metric coefficients  $\alpha, \beta^j, g_{jk}$  are the lapse, shift, and 3-metric functions. These functions are given by

$$\begin{aligned} \alpha &= \left(\frac{\Sigma\Delta}{A}\right)^{1/2}, & g_{rr} &= \frac{\Sigma}{\Delta}, & g_{\theta\theta} &= \Sigma, & g_{\varphi\varphi} &= \frac{\sin^2\theta A}{\Sigma} \\ \beta^\varphi &= -\omega = -\frac{2Mar}{A}, & \beta^j &= g_{jk} = 0 & & & & \text{for all other } j \text{ and } k, \end{aligned}$$

where  $M$  is the mass of the black hole,  $a$  is its angular momentum per unit mass, and the functions  $\Delta, \Sigma, A$  are defined by

$$\Delta = r^2 - 2Mr + a^2, \quad \Sigma = r^2 + a^2 \cos^2\theta, \quad A = (r^2 + a^2)^2 - a^2\Delta \sin^2\theta.$$

We introduce a set of local observers who rotate with the Keplerian angular velocity. Each observer carries an orthonormal tetrad. For the Keplerian orbiting observer with a coordinate angular velocity of  $\Omega$ , its world line is  $r = \text{constant}$ ,  $\theta = \text{constant}$ ,  $\varphi = \Omega t + \text{constant}$ . The observer in the LNRF who rotates with the angular velocity  $\omega$  measures the linear velocity of a particle moving in a Keplerian orbit as  $v_{(\varphi)} = dx^{(\varphi)}/dx^{(0)} = \alpha^{-1}\sqrt{g_{\varphi\varphi}}(\Omega - \omega)$  where  $x^{(0)}$  and  $x^{(\varphi)}$  are the time and spatial coordinates in LNRF. Its Lorentz factor is  $\gamma = (1 - v_{(\varphi)}^2)^{-1/2}$ . We adopt the orbiting frame with the set of its basis vectors:

$$\mathbf{e}_{\hat{0}} = \gamma e^{-\nu} \left( \frac{\partial}{\partial t} + \Omega \frac{\partial}{\partial \varphi} \right), \quad \mathbf{e}_{\hat{\varphi}} = \gamma \left( e^{-\psi} \frac{\partial}{\partial \varphi} + v_{(\varphi)} e^{-\nu} \left( \frac{\partial}{\partial t} + \omega \frac{\partial}{\partial \varphi} \right) \right), \quad (2)$$

$$\mathbf{e}_{\hat{r}} = e^{-\mu_1} \frac{\partial}{\partial r}, \quad \mathbf{e}_{\hat{\theta}} = e^{-\mu_2} \frac{\partial}{\partial \theta}, \quad (3)$$

where  $e^\nu, e^\psi, e^{\mu_1}, e^{\mu_2}$  are defined by

$$e^\nu = \alpha, \quad e^{2\psi} = g_{\varphi\varphi}, \quad e^{2\mu_1} = g_{rr}, \quad e^{2\mu_2} = g_{\theta\theta}. \quad (4)$$

The corresponding orthogonal basis of one-forms is

$$\begin{aligned} \vec{\omega}^{\hat{t}} &= \hat{\alpha} \mathbf{d}t - v_{(\varphi)} \gamma e^\psi \mathbf{d}\varphi, & \vec{\omega}^{\hat{\varphi}} &= -\Omega \gamma e^\psi \mathbf{d}t + \gamma e^\psi \mathbf{d}\varphi \\ \vec{\omega}^{\hat{r}} &= e^{\mu_1} \mathbf{d}r, & \vec{\omega}^{\hat{\theta}} &= e^{\mu_2} \mathbf{d}\theta. \end{aligned} \quad (5)$$

Here  $\hat{\alpha}$  is defined by  $\hat{\alpha} = \alpha\gamma(1 + v_\omega v_{(\varphi)})$ , where  $v_\omega$  is the "rotating velocity of the geometry of spacetime",  $v_\omega = \omega e^{\psi-\nu}$ . The rotation one-forms,  $\omega_{\hat{b}}^{\hat{a}}$ , which allow one to read off the connection coefficients  $\Gamma_{\hat{b}\hat{i}}^{\hat{a}}$  by  $\omega_{\hat{b}}^{\hat{a}} = \Gamma_{\hat{b}\hat{i}}^{\hat{a}} \vec{\omega}^{\hat{i}}$ . Hereafter the components of the tensor in the orbiting frame are depicted by the superscript with hat. The connection coefficients  $\Gamma_{\hat{b}\hat{i}}^{\hat{a}}$  are represented in Appendix A.

The Maxwell equations for the electromagnetic field  $F^{\hat{\mu}\hat{\nu}}$  produced by a four current density  $J^{\hat{\mu}}$  are

$$F_{;\hat{\mu}}^{\hat{\mu}\hat{\nu}} = -J^{\hat{\nu}}, \quad F_{\hat{\mu}\hat{\nu};\hat{\lambda}} + F_{\hat{\lambda},\hat{\mu};\hat{\nu}} + F_{\hat{\nu}\hat{\lambda};\hat{\mu}} = 0. \quad (6)$$

In the orbiting frame they are represented as follows:

$$\begin{aligned} \frac{\partial \mathbf{B}}{\partial \hat{\tau}} + \frac{1}{\hat{\alpha}} \nabla \times (\hat{\alpha} \mathbf{E}) \\ - \mathbf{n}_{\hat{\varphi}} e^b v_\Omega \mathbf{B} \cdot \nabla \ln \Omega - e^b \mathbf{v}_{(\varphi)} \cdot \mathbf{B} \nabla \ln \hat{\alpha} - \gamma^2 v_{(\varphi)} v_\Omega \mathbf{E} \times \nabla \ln (\Omega/\hat{\alpha}) = 0, \end{aligned} \quad (7)$$

$$\begin{aligned} \frac{\partial \mathbf{E}}{\partial \hat{\tau}} - \frac{1}{\hat{\alpha}} \nabla \times (\hat{\alpha} \mathbf{B}) \\ - \mathbf{n}_{\hat{\varphi}} e^b v_\Omega \mathbf{E} \cdot \nabla \ln \Omega - e^b \mathbf{v}_{(\varphi)} \cdot \mathbf{E} \nabla \ln \hat{\alpha} - \gamma^2 v_{(\varphi)} v_\Omega \mathbf{B} \times \nabla \ln (\Omega/\hat{\alpha}) = -\frac{4\pi}{c} \mathbf{J}, \end{aligned} \quad (8)$$

$$\nabla \cdot \mathbf{E} - v_{(\varphi)} \mathbf{E} \cdot \nabla \Omega + e^b \mathbf{v}_{(\varphi)} \cdot (\mathbf{B} \times \nabla) \ln \hat{\alpha} = \frac{4\pi}{c} J^{\hat{0}}, \quad (9)$$

$$\nabla \cdot \mathbf{B} - v_{(\varphi)} \vec{\mathbf{B}} \cdot \nabla \Omega - e^b \mathbf{v}_{(\varphi)} \cdot (\mathbf{E} \times \nabla) \ln \hat{\alpha} = 0. \quad (10)$$

Here  $d\hat{\tau}$  is the variation of time in the orbiting frame and it combines with the corresponding time  $dt$  in the static frame by  $d\hat{\tau} = \gamma^{-1} \alpha dt$ . The symbol  $\mathbf{n}_{\hat{i}}$  is the unit vector in the  $\hat{i}$  direction in the space of the orbiting frame. The vectors  $\mathbf{B} = B^{\hat{i}} \mathbf{n}_{\hat{i}}$  and  $\mathbf{E} = E^{\hat{i}} \mathbf{n}_{\hat{i}}$  are the magnetic and electric fields with components  $E^{\hat{r}} = F^{\hat{0}\hat{r}}$ ,  $B^{\hat{\varphi}} = F^{\hat{r}\hat{\theta}}$ , and so on. The symbol  $\nabla$  is the covariant derivative operator, and  $\mathbf{v}_{(\varphi)}$ ,  $v_\Omega$  and  $e^b$  are defined by  $\mathbf{v}_{(\varphi)} = v_{(\varphi)} \mathbf{n}_{\hat{\varphi}}$ ,  $v_\Omega = \Omega e^{\psi-\nu}$  and  $e^b = \gamma^2(1 + v_{(\varphi)} v_\omega)$ . When the angular velocity of the frame is taken to be the geometrical angular velocity,  $\Omega \rightarrow \omega$ , the above expressions of Maxwell equations (7)–(10) result in the forms described in LNRF (Thorne & Macdonald 1982; Thorne et al. 1986).

The Lorentz force is represented by

$$\frac{1}{c} \mathbf{J} \times \mathbf{B} = -\nabla \frac{(\hat{\alpha} B)^2}{8\pi \hat{\alpha}} + \frac{1}{4\pi} \mathbf{B} \cdot \nabla (\hat{\alpha} \mathbf{B}) + \gamma^2 v_{(\varphi)} v_\Omega \left( -\frac{B^2}{4\pi} \nabla + \frac{\mathbf{B}}{4\pi} \mathbf{B} \cdot \nabla \right) \ln(\hat{\alpha}/\Omega). \quad (11)$$

The energy-momentum tensor in LNRF,  $T^{(i)(j)}$ , is expressed with the four velocity of fluid  $u^{(i)}$ , the pressure  $P$ , and the density  $\rho$  as

$$T^{(i)(j)} = (\rho + P) u^{(i)} u^{(j)} + \eta^{(i)(j)} P. \quad (12)$$

Hereafter the components of a tensor in LNRF are expressed by the superscript with the parenthesis. The tensor  $\eta^{(i)(j)}$  is the Minkowskian metric. The Euler equations with the Lorentz force,  $F^{(i)(\nu)}J_{(\nu)}$ , are represented by

$$\frac{\partial(\rho + P)u^{(0)}u^{(i)}}{\partial\tilde{\tau}} + \frac{1}{\alpha}\tilde{\nabla} \cdot \alpha(\rho + P)\mathbf{u}u^{(i)} + \frac{1}{\alpha}\tilde{\nabla}\alpha P + \Gamma_{(\mu)(\nu)}^{(i)}T^{(\mu)(\nu)} = F^{(i)(\nu)}J_{(\nu)}, \quad (13)$$

where  $\tilde{\tau}$  and  $\tilde{\nabla}$  are the time and the covariant derivative operator in LNRF. The variation of time,  $d\tilde{\tau}$ , is combined with  $d\hat{\tau}$  by  $d\tilde{\tau} = \gamma d\hat{\tau}$ . The Lorentz force is related likewise as  $F^{(i)(\nu)}J_{(\nu)} = \gamma F^{\hat{i}\hat{\nu}}J_{\hat{\nu}}$ . The term  $\Gamma_{(\mu)(\nu)}^{(i)}T^{(\mu)(\nu)}$  is the "inertial force" in the  $(i)$  direction. The forces for  $(i) = (r), (\theta)$  are expressed in explicit forms:

$$\begin{aligned} \Gamma_{(\mu)(\nu)}^{(i)}T^{(\mu)(\nu)} &= T^{(0)(0)}\tilde{\nabla}^{(i)}\ln\alpha + T^{(0)(\varphi)}v_{\omega}\tilde{\nabla}^{(i)}\ln\omega - T^{(\varphi)(\varphi)}\tilde{\nabla}^{(i)}\psi \\ &+ T^{(i)(j)}\tilde{\nabla}^{(j)}\mu_i - T^{(j)(j)}\tilde{\nabla}^{(i)}\mu_j. \end{aligned} \quad (14)$$

Here the  $(r)$  component of  $T^{(i)(j)}\tilde{\nabla}^{(j)}\mu_i - T^{(j)(j)}\tilde{\nabla}^{(i)}\mu_j$  is  $T^{(r)(\theta)}\tilde{\nabla}^{(\theta)}\mu_1 - T^{(\theta)(\theta)}\tilde{\nabla}^{(r)}\mu_2$ , and the  $(\theta)$  component is  $T^{(\theta)(r)}\tilde{\nabla}^{(r)}\mu_2 - T^{(r)(r)}\tilde{\nabla}^{(\theta)}\mu_1$ . The  $(\varphi)$  component of the "inertial force" is

$$\Gamma_{(\mu)(\nu)}^{(\varphi)}T^{(\mu)(\nu)} = (\rho + p)u^{(\varphi)}\mathbf{u} \cdot \tilde{\nabla}\psi. \quad (15)$$

This term is correspond to the "Coliori's force".

The equation of continuity is

$$\frac{\partial\rho u^{(0)}}{\partial\tilde{\tau}} + \frac{1}{\alpha}\tilde{\nabla} \cdot \alpha\rho\mathbf{u} = 0, \quad (16)$$

### 3. Groth Rates of Magnetorotational Instability

#### 3.1. Dispersion Relation

The magnetohydrodynamical variables are expanded by the infinitesimal quantities,  $\mathbf{v} = \mathbf{v}_0 + \delta\mathbf{v}$ ,  $\mathbf{B} = \mathbf{B}_0 + \delta\mathbf{B}$ ,  $\rho = \rho_0 + \delta\rho$  and  $P = P_0 + \delta P$ . We assume the axisymmetric perturbations and use the local WKB approximation. The variables are unified to be the components in the orbiting frame by the transformations of the hydrodynamic equations from LNRF to the orbiting frame. The linearized equations are then described by

$$\begin{aligned} \nabla \cdot \delta\mathbf{v} &= 0, \\ \frac{\partial\delta v^{\hat{r}}}{\partial\hat{\tau}} &- 2\tilde{\Omega}_{\hat{r}}\delta v^{\hat{\varphi}} + \frac{1}{\gamma\rho}\frac{\partial\delta P}{\partial x^{\hat{r}}} - \frac{\delta\rho}{\gamma\rho^2}\frac{\partial P}{\partial x^{\hat{r}}} \end{aligned} \quad (17)$$

$$+ \frac{1}{4\pi\rho} \left( B^{\hat{\theta}} \frac{\partial \delta B^{\hat{\theta}}}{\partial x^{\hat{r}}} - B^{\hat{\theta}} \frac{\partial \delta B^{\hat{r}}}{\partial x^{\hat{\theta}}} + 2B^{\hat{\theta}} \delta B^{\hat{\theta}} \gamma^2 v_{(\varphi)} v_{\Omega} \nabla^{\hat{r}} \ln(\hat{\alpha}/\Omega) \right) = 0, \quad (18)$$

$$\frac{\partial \delta v^{\hat{\theta}}}{\partial \hat{r}} - 2\tilde{\Omega}_{\hat{\theta}} \delta v^{\hat{\varphi}} + \frac{1}{\gamma\rho} \frac{\partial \delta \rho}{\partial x^{\hat{\theta}}} - \frac{\delta \rho}{\gamma\rho^2} \frac{\partial P}{\partial x^{\hat{\theta}}} = 0, \quad (19)$$

$$\frac{\partial \delta v^{\hat{\varphi}}}{\partial \hat{r}} + \vec{\kappa} \cdot \delta \mathbf{v} - \frac{1}{4\pi\rho} B^{\hat{\theta}} \frac{\partial \delta B^{\hat{\varphi}}}{\partial x^{\hat{\theta}}} = 0, \quad (20)$$

$$\frac{\partial \delta B^{\hat{r}}}{\partial \hat{r}} - \mathbf{B} \cdot \nabla \delta v^{\hat{r}} = 0, \quad (21)$$

$$\frac{\partial \delta B^{\hat{\theta}}}{\partial \hat{r}} - \mathbf{B} \cdot \nabla \delta v^{\hat{\theta}} - B^{\hat{\theta}} \delta v^{\hat{r}} \gamma^2 v_{(\varphi)} v_{\Omega} \nabla^{\hat{r}} \ln(\hat{\alpha}/\Omega) = 0, \quad (22)$$

$$\frac{\partial \delta B^{\hat{\varphi}}}{\partial \hat{r}} - \mathbf{B} \cdot \nabla \delta v^{\hat{\varphi}} - \gamma^2 v_{\Omega} \delta \mathbf{B} \cdot \nabla \ln \Omega = 0, \quad (23)$$

$$\frac{5}{3\rho} \frac{\partial \delta \rho}{\partial \hat{r}} + \delta v^{\hat{r}} \frac{\partial \ln P \rho^{-5/3}}{\partial x^{\hat{r}}} + \delta v^{\hat{\theta}} \frac{\partial \ln P \rho^{-5/3}}{\partial x^{\hat{\theta}}} = 0, \quad (24)$$

where the coefficients  $\vec{\tilde{\Omega}} = (\tilde{\Omega}_{\hat{r}}, \tilde{\Omega}_{\hat{\theta}})$  and  $\vec{\kappa} = (\kappa_{\hat{r}}, \kappa_{\hat{\theta}})$  are defined by

$$\vec{\tilde{\Omega}} = \gamma(v_{(\varphi)} \nabla \psi - \frac{1}{2} v_{\omega} \nabla \ln \omega), \quad \text{and} \quad \vec{\kappa} = \gamma v_{(\varphi)} \nabla \ln(\gamma^2 e^{\psi} v_{(\varphi)}). \quad (25)$$

With the spacetime dependence of perturbations,  $e^{i(k_{\hat{r}}x^{\hat{r}} + k_{\hat{\theta}}x^{\hat{\theta}} - \hat{\Gamma}\hat{r})}$ , the explicit dispersion relation is derived as

$$\begin{aligned} \frac{k^2}{k_{\hat{\theta}}^2} \check{\Gamma}^4 - \left[ \kappa^2 + \left( \frac{k_{\hat{r}}}{k_{\hat{\theta}}} N_{\hat{\theta}} - N_{\hat{r}} \right)^2 \right] \check{\Gamma}^2 - (\kappa^2 + \chi^2) (\mathbf{k} \cdot \mathbf{v}_A)^2 \\ + v_A^2 \gamma^2 v_{(\varphi)} v_{\Omega} \nabla^{\hat{r}} \ln(\Omega/\hat{\alpha}) \left( 2\gamma^2 v_{(\varphi)} v_{\Omega} \nabla^{\hat{r}} \ln(\Omega/\hat{\alpha}) - i3k_{\hat{r}} \right) \frac{(\mathbf{k} \cdot \mathbf{v}_A)^2}{(k_{\hat{\theta}} v_A)^2} \check{\Gamma}^2 = 0, \end{aligned} \quad (26)$$

where

$$\check{\Gamma}^2 = \hat{\Gamma}^2 - (\mathbf{k} \cdot \mathbf{v}_A)^2, \quad k^2 = k_{\hat{r}}^2 + k_{\hat{\theta}}^2, \quad N_i^2 = -\frac{3}{5\gamma\rho} \frac{\partial P}{\partial x^{\hat{i}}} \frac{\partial \ln P \rho^{-5/3}}{\partial x^{\hat{i}}} \quad \text{for } \hat{i} = \hat{r}, \hat{\theta}, \quad (27)$$

and

$$\kappa^2 = 2 \left( \tilde{\Omega}_{\hat{r}} - \frac{k_{\hat{r}}}{k_{\hat{\theta}}} \tilde{\Omega}_{\hat{\theta}} \right) \left( \kappa_{\hat{r}} - \frac{k_{\hat{r}}}{k_{\hat{\theta}}} \kappa_{\hat{\theta}} \right), \quad \chi^2 = -2\gamma^2 v_{\Omega} \left( \tilde{\Omega}_{\hat{r}} - \frac{k_{\hat{r}}}{k_{\hat{\theta}}} \tilde{\Omega}_{\hat{\theta}} \right) \left( \nabla^{\hat{r}} - \frac{k_{\hat{r}}}{k_{\hat{\theta}}} \nabla^{\hat{\theta}} \right) \ln \Omega. \quad (28)$$

### 3.2. Growth Rates

The dispersion relation (26) has the resemblant form to a Newtonian case except the last term. When  $v_A^2 \ll N^2 = N_{\hat{r}}^2 + N_{\hat{\theta}}^2$ , i.e., the magnetic pressure is negligibly small in

comparison with the gas pressure,  $\beta = P_{gass}/P_{mag} \gg 1$ , the last term containing  $v_A^2 \gamma^2 v_{(\varphi)} v_\Omega$  can be ignored in (26). At the equatorial plane and far from a black hole, the functions,  $\kappa^2$  and  $\chi^2$ , have the following forms:

$$\kappa^2 \rightarrow \frac{2\Omega}{r} \frac{(r^2\Omega)}{\partial r}, \quad \chi^2 \rightarrow -\frac{\partial\Omega^2}{\partial \ln r}. \quad (29)$$

The equation (26) then coincides with a Newtonian dispersion relation (Balbus & Hawley 1991). The equation (26) is the general dispersion relation of MRI for all radii and for all  $a$ .

In the Newtonian case, the maximum growth rate relative to a angular velocity of a circular orbit,  $\Gamma_{max}/\Omega$ , has an universal value in all radii and in all mass scales of a central object (Balbus & Hawley 1991). Here we introduce the angular velocity of a circular orbit measured in LNRF,  $\tilde{\Omega} = (\Omega - \omega)/\alpha$ . At the next it is transferred into the orbiting frame as  $\hat{\Omega} = \gamma\tilde{\Omega} = (\Omega - \omega)\gamma/\alpha$ . It may be said that  $-\hat{\Omega}$  is the proper angular velocity of the geometry measured in the orbiting frame. Let's consider first a simple case for  $\beta \ll 1$ ,  $k_{\hat{r}} = B^{\hat{r}} = 0$ , and introduce the dimensionless variables with use of a angular velocity  $\hat{\Omega}$  as

$$\bar{\Gamma} = \hat{\Gamma}/\hat{\Omega}, \quad \bar{k} = (\mathbf{k} \cdot \mathbf{v}_A)/\hat{\Omega}, \quad \bar{N} = N_{\hat{r}}/\hat{\Omega}, \quad \bar{\Omega}_{\hat{r}} = \tilde{\Omega}_{\hat{r}}/\hat{\Omega}, \quad \bar{\kappa} = \kappa/\hat{\Omega}, \quad \text{and} \quad \bar{\chi} = \chi/\hat{\Omega}^2. \quad (30)$$

Here it may be noticed that the dimensionless growth rate  $\bar{\Gamma}$  coincides with that in LNRF,  $\bar{\Gamma} = \hat{\Gamma}/\hat{\Omega} = \tilde{\Gamma}/\tilde{\Omega}$ , where  $\tilde{\Gamma}$  is the growth rate measured in LNRF,  $\tilde{\Gamma} = -id \ln \delta / d\tilde{\tau}$ . The disk is assumed to be isothermal and the Brunt-Väisälä frequency is taken to be  $\bar{N}_\theta^2 = N_\theta^2/\hat{\Omega}^2 = 0.8$  and  $\bar{N}_{\hat{r}}^2 = N_{\hat{r}}^2/\hat{\Omega}^2 = 0.01\bar{N}_\theta^2$ .

The dispersion relation (26) will lead to instability for values of  $\bar{k}$  less than the critical value:

$$\bar{k}_{crit}^2 = \bar{\chi}^2 - \bar{N}^2. \quad (31)$$

The unstable mode of a perturbation has a maximum growth rate,  $\hat{\Gamma}_{max}$ , at the wavenumber,  $\bar{k} = \bar{k}_{max}$  such as

$$\hat{\Gamma}_{max}^2 = -\frac{\chi^2}{4} \frac{(1 - \bar{N}^2/\bar{\chi}^2)^2}{1 + \bar{\kappa}^2/\bar{\chi}^2}, \quad \text{and} \quad \bar{k}_{max}^2 = \frac{\bar{\chi}^2}{4} \frac{1 - \bar{N}^2/\bar{\chi}^2}{1 + \bar{\kappa}^2/\bar{\chi}^2} (1 + (2\bar{\kappa}^2 + \bar{N}^2)/\bar{\chi}^2). \quad (32)$$

When  $a = M$ , the asymptotic behaviors of the proper growth rate  $\hat{\Gamma}_{max}(r)$  and wavenumber  $\bar{k}_{max}(r)$  for  $r \rightarrow r_{ms}$  are simply expressed by the asymptotic relation between  $\Omega(r)$  and  $\omega(r)$ . We show in Fig. 2 the variations of dimensionless variables,  $\bar{\chi}^2$ ,  $\bar{\kappa}^2$  and  $\bar{\Gamma}_{max}^2$ ,  $\bar{k}_{max}$ , along the radius from a event horizon for  $a = M, 0$ . When  $r \rightarrow r_{ms}$  and  $a \rightarrow M$ , the angular velocity of a circular orbit coincides with the geometrical angular velocity,  $\Omega \rightarrow \omega$ . The "Coliori's force"  $\kappa^{\hat{r}} \delta v^{\hat{r}}$  in (20) then reduces to be zero,  $\kappa^{\hat{r}} \delta v^{\hat{r}} \propto v_{(\varphi)} \nabla^{\hat{r}} \ln(\gamma^2 e^\psi v_{(\varphi)}) = (\Omega - \omega) A r^{-3} \nabla^r \ln(\gamma^2 e^\psi v_{(\varphi)}) \rightarrow 0$  for  $r \rightarrow r_{ms}$ . Thus the epicyclic frequency,  $\kappa = (2\tilde{\Omega}_{\hat{r}} \kappa_{\hat{r}})^{1/2}$ ,



becomes to be zero. Since  $\bar{\chi}^2 \geq 2$ , the ratio  $\bar{N}^2/\bar{\chi}^2$  is negligibly small in (32). The maximum growth rate  $\hat{\Gamma}_{max}$  and wavenumber  $\bar{k}_{max}$  at  $r \approx r_{ms}$  are then simply expressed as,

$$\hat{\Gamma}_{max}^2 \approx -\frac{\chi^2}{4} \quad \bar{k}_{max}^2 \approx \frac{\bar{\chi}^2}{4}. \quad (33)$$

The value of  $\chi^2$  is determined by the strengths of two actions. One is the radial acceleration  $\delta v^{\hat{r}}$  by the "centrifugal force",  $\delta v^{\hat{r}} \propto 2\tilde{\Omega}_{\hat{r}}\delta v^{\hat{\phi}}$ . Other is the induction of magnetic field by the differential rotation of fluid motion,  $\delta B^{\hat{\phi}} \propto \delta B^{\hat{r}}\gamma^2 v_{\Omega}\nabla^{\hat{r}}\ln\Omega$ . We define the shear term by  $\Omega_{shear} = \gamma^2 v_{\Omega}\nabla^{\hat{r}}\ln(\Omega)$ . Then the function  $\chi^2$  is expressed as  $\chi^2 = -2\tilde{\Omega}_{\hat{r}}\Omega_{shear}$ . The asymptotic forms of  $\Omega_{shear}$  and  $\tilde{\Omega}_{\hat{r}}$  are represented as  $\Omega_{shear} = -1.5\Omega$  and  $\tilde{\Omega}_{\hat{r}} = \Omega$  for  $r \rightarrow \infty$ , and  $\Omega_{shear} = -4\Omega$  and  $\tilde{\Omega}_{\hat{r}} = -2\gamma\nabla^r\omega = (4/\sqrt{3})\omega$  for  $r \rightarrow r_{ms}$ . The efficiencies of the two actions relative to the angular velocity  $\Omega$  or the proper angular velocity  $\hat{\Omega}$ (see Fig. 2) are increased at  $r \approx r_{ms}$ . When  $r \rightarrow r_{ms}$ , the function  $\tilde{\Omega}_{\hat{r}}$  in (25) is represented mainly by the variable related with the differential rotation of the geometry,  $v_{\omega}\nabla^{\hat{r}}\ln\omega$ , since another variable  $v_{(\varphi)}\nabla^{\hat{r}}\psi$  reduces to be zero,  $v_{(\varphi)}\nabla^{\hat{r}}\psi = (\Omega - \omega)e^{\psi-\nu}\nabla^{\hat{r}}\psi = (\Omega - \omega)Ar^{-3}\nabla^r\psi \rightarrow 0$ . The finite values of the growth rate  $\hat{\Gamma}_{max}$  and of the wavenumber  $\bar{k}_{max}$  at  $r = r_{ms}$  are realized by the rotation of the geometry.

The maximum amplitude of the proper growth rate  $|\hat{\Gamma}_{max}(r)|$  increases in the similitude of the Newtonian angular velocity of a circular orbit  $\Omega_N = 3/4(Mr^{-3})^{1/2}$  for  $r \rightarrow r_{ms}$ . We show in Fig. 1 the amplitudes of growth rates  $|\hat{\Gamma}_{max}(r)|$  for  $a = M, 0$ . The ratio  $|\hat{\Gamma}_{max}(r)|/(3/4(Mr^{-3})^{1/2})$  is restricted to a finite range as pointed by Gammie (2004). Here its ratio varies between 1 and  $5/(2\sqrt{3}) \approx 1.44$  when  $r \geq r_{ms}$  and  $v_A < 0.1c$ . The rapidly rotating black hole with  $a = M$  produces the rapid growth rate which is about one-order of magnitude larger than that for  $a = 0$ ,  $\hat{\Gamma}_{max}(r_{ms}, a = M) = 12.5\hat{\Gamma}_{max}(r_{ms}, a = 0)$ . If the marginally bound orbit  $r_{mb}$  or photon orbit  $r_{ph}$  is realized for  $a = 0$ , then the proper growth rate  $|\hat{\Gamma}_{max}|$  reaches to  $\infty$ .

It is useful for the magnetohydrodynamics to evaluate the growth rate in MRI in comparison with the speeds of other dynamical processes. The angular velocity of a circular orbit  $\hat{\Omega}$  is a typical measure to make clear the characteristic speeds of the growth rates,  $\bar{\Gamma} = \hat{\Gamma}/\hat{\Omega}$ , and to make clear the typical wavelength of perturbations,  $\bar{k}_{max} = (\mathbf{k} \cdot \mathbf{v}_A)/\hat{\Omega}$ . We show in Fig. 3 the dispersion relations with use of  $\bar{\Gamma}$  and  $\bar{k}$  for  $a = M, 0$ . In the rapidly rotating spacetime with  $a = M$ , the relative growth rate  $\bar{\Gamma}$  is observed to be very large in the vicinity of  $r_{ms}$ . Its relative value reaches to  $|\bar{\Gamma}(r \approx r_{ms})| \approx 3.75 \approx 5|\bar{\Gamma}(r = \infty)|$ . The unstable range of wavenumber  $\bar{k}_{crit}$  is measured to expand in proportion to the shear variable  $\bar{k}_{crit} \propto \bar{\chi}$ . On the other hand the relative growth rates  $\bar{\Gamma}(r)$  and the critical wavenumbers  $\bar{k}_{crit}$  in the static spacetime  $a = 0$  little change at the space  $r \geq r_{ms}$ . These characteristic asymptotic behaviors of the relative quantities,  $\bar{\Gamma}_{max}(r \rightarrow r_{ms})$  and  $\bar{k}_{crit}$ , are brought about partially by

the variations of  $\hat{\Omega}(r \rightarrow r_{ms})$ . When  $a = 0$  and  $r \rightarrow r_{ms}$ , the circular velocity  $v_{\Omega}(r)$  and the proper angular velocity  $\hat{\Omega}(r)$  increase in inverse proportion to  $(r - r_h)^n$ , while for  $a = M$ , the circular velocity  $v_{(\varphi)}(r)$  and the proper angular velocity  $\hat{\Omega}(r)$  become constant at  $r \approx 2r_{ms}$ . The rapid rotation of the geometry restricts the increases of  $v_{(\varphi)}(r)$  and  $\hat{\Omega}(r)$  for  $r \rightarrow r_{ms}$  to be  $v_{(\varphi)} = v_{\Omega} - v_{\omega} = \infty - \infty \rightarrow 1/2$  and  $\hat{\Omega} = \gamma\Omega e^{-\nu} - \gamma\omega e^{-\nu} = \infty - \infty \rightarrow 1/(2\sqrt{3})$ . The observers in LNRF(ZAMOs) evaluate the growth rate  $\tilde{\Gamma}$  to be large in comparison with the observed angular velocity of a circular motion  $\tilde{\Omega}$ .

Let's consider the dispersion relation over the extended space around a black hole. The rotating black hole distorts the geometry of spacetime not only in the radial direction but also in the azimuthal direction. The angular velocity of a circular orbit at a finite height  $z$  from the equatorial plane,  $\Omega(r, z)$ , was represented by Yokosawa, Uematsu & Abe (2004). They assumed the pressure force in the vertical direction to be balanced with the gravity. By using its angular velocity,  $\Omega(r, z)$ , the dispersion relation on the plane,  $z = \text{constant}$ , is obtained. Here we introduce the cylindrical spatial coordinates  $(\varpi, z, \varphi)$  where  $\varpi$  and  $z$  are defined by  $\varpi = r \sin \theta, z = r \cos \theta$ . The derivative in  $\hat{\varpi}$  or  $\hat{z}$  direction is given by the combination of the components of the derivatives in  $\hat{r}$  and  $\hat{\theta}$  directions, e.g.,  $\nabla^{\hat{\varpi}}\Omega = \sin \theta \nabla^{\hat{r}}\Omega + \cos \theta \nabla^{\hat{\theta}}\Omega$ . The distributions of the maximum amplitude of the growth rate,  $\bar{\Gamma}_{max}^2(\varpi, z)$ , and the wavenumber at the maximum growth rate,  $\bar{k}_{max}(\varpi, z)$ , are depicted in Fig.4, where the Brunt-Väisälä frequency is assumed to be constant,  $\bar{N}_z^2 = N_z^2/\hat{\Omega}^2 = 0.8$  and  $\bar{N}_{\varpi}^2 = 0.01\bar{N}_z^2$ , and the directions of magnetic field and wavenumber are fixed to be  $\mathbf{B} = B^z \mathbf{n}_z$  and  $\mathbf{k} = k_z \mathbf{n}_z$ . When  $a = M$ , the amplitude of the maximum growth rate,  $\bar{\Gamma}_{max}^2(\varpi, z)$ , is large over the wide area around a black hole. The wavenumber  $\bar{k}_{max}(\varpi, z)$  greatly increases near to the event horizon.

### 3.3. Magnetorotational Instability exerted by the Magnetic Fields Induced by the Differential Rotation of the Orbiting Frame

When  $\beta \leq 1$  and  $\gamma^2 v_{\Omega} v_{(\varphi)} / c^2 \approx 1$ , the term containing  $v_A^2 \gamma^2 v_{(\varphi)} v_{\Omega}$  in the dispersion relation (26) exerts on the MRI. When  $k_{\hat{r}} = 0$ , the insertion of this term leads to no change of wave mode in the characteristics of perturbations. The sign of this term is contradictory to the sign of the change in fluid  $N^2$ , which means that this term enhances the MRI. The dispersion relation for  $a = M, r = 1.001r_{ms}, z = 0$  and  $k_{\hat{r}} = 0$  is shown in Fig.5. When Alfvén velocity  $v_A$  is larger than  $\sim 0.1c$ , the growth rate is remarkably enhanced by this term and the perturbations with  $\bar{k} = 0$  become unstable,  $\Gamma^2(k = 0) < 0$ .

When the wave is propagating in the radial direction,  $\delta \propto e^{\Gamma_R t + i(\Gamma_I t + k_{\hat{r}} x^{\hat{r}} + k_{\hat{\theta}} x^{\hat{\theta}})}$ , the waves of perturbations become over stable. The unstable branch of the dispersion relation in phase space  $(k_{\hat{\theta}}, k_{\hat{r}})$  is shown in Fig.7, where the parameters are set to be  $v_A = 0.5c, a = M, r =$

$1.001r_{ms}$  and  $z = 0$ . Here the direction of magnetic field is fixed to be  $\mathbf{B} = B^{\hat{\theta}}\mathbf{n}_{\hat{\theta}}$ . The imaginary component of the growth rate  $\Gamma_I$  is also shown in Fig.7. The wave frequency  $\Gamma_I$  increases in accordance with the radial wavenumber  $k_{\hat{r}}$ . When the Alfvén velocity is nonrelativistic,  $v_A \ll c$ , the unstable branch in the wavenumber space  $(k_{\hat{\theta}}, k_{\hat{r}})$  is restricted in a area  $k_{\hat{\theta}}^2 + k_{\hat{r}}^2 \leq k_{crit}^2$  (see the left pannel in Fig.6). Here  $\Gamma_I \approx 0$  (see the right panel in Fig.6), and then the perturbations exponentially grow. When  $v_A \geq 0.1c$ , the unstable area of the phase space  $(k_{\hat{\theta}}, k_{\hat{r}})$  enlarges to the larger radial wave number,  $k_{\hat{r}} > k_{crit}$  (Fig.7). The oscillating waves exponentially increase their amplitudes over the wide space of wavenumbers  $(k_{\hat{\theta}}, k_{\hat{r}})$ .

The above instability is caused by the magnetic induction due to the differential rotation of the orbiting frame,

$$\frac{\partial \mathbf{B}}{\partial \hat{t}} \propto -\gamma^2 v_{(\varphi)} v_{\Omega} (\mathbf{v} \times \mathbf{B}) \times \nabla \ln(\Omega/\hat{\alpha}). \quad (34)$$

The perturbation of a radial velocity  $\delta v^{\hat{r}}$  exponentially increases the magnetic field,

$$\frac{\partial \ln B^{\hat{\theta}}}{\partial \hat{t}} \propto -\gamma^2 v_{(\varphi)} v_{\Omega} \delta v^{\hat{r}} \nabla^{\hat{r}} \ln(\Omega/\hat{\alpha}) > 0, \quad \text{when } \delta v^{\hat{r}} > 0. \quad (35)$$

The increased magnetic field more enhances the motion of fluid according to the equations (18)—(20).

#### 4. Discussion

Balbus & Hawley (1992) had shown that the maximum growth rate of MRI agrees with the local Oort  $A$ -value of the disk. It is conjectured that the Oort  $A$ -value of a disk is an upper bound to the growth rate of any instability feeding upon the free energy of differential rotation. They have investigated the reasons behind this remarkably general behavior of MRI by using a form of the dynamical Hill equations (Hill 1878). The Hill equations have found their widest applicability in the study of collisionless system. We show here that the maximum growth rate of MRI in curved spacetime is somewhat different from the general relativistic version analogous to the local Oort  $A$ -value.

The local Oort  $A$ -value is the growth rate of the dynamical shear instability of a particle motion in the field of central potential. Its instability is caused by the displacement of the particle orbit in which the angular velocity of a circular orbit keeps a original value,  $\Omega = \Omega_0$ . When the displacement is positive, i.e.  $\delta r > 0$ , the centrifugal force is then superior to the gravitational force, the radius of the perturbed orbit becomes more larger, and vice versa.

When the motion is restricted in the equatorial plane, the geodesic equations in LNRF are represented with the expressions of the time coordinate,  $dx^{(0)} = d\tilde{t}$ , and the covariant

derivative,  $\tilde{\nabla}^{(r)}$ , as

$$\frac{d^2 x^{(r)}}{d\tilde{\tau}^2} + \tilde{\nabla}^{(r)} \ln \alpha + v_\omega \frac{dx^{(\varphi)}}{d\tilde{\tau}} \tilde{\nabla}^{(r)} \ln \omega - \left( \frac{dx^{(\varphi)}}{d\tilde{\tau}} \right)^2 \tilde{\nabla}^{(r)} \ln e^\psi = 0, \quad (36)$$

$$\frac{d^2 x^{(\varphi)}}{d\tilde{\tau}^2} + \frac{dx^{(\varphi)}}{d\tilde{\tau}} \frac{dx^{(r)}}{d\tilde{\tau}} \tilde{\nabla}^{(r)} \ln e^\psi = 0. \quad (37)$$

Let's consider the situation of perturbations that the particle is allowed to make small excursions from a circular orbit,  $x^{(r)} = e^{\mu_1} R_0$ ,  $dx^{(\varphi)} = e^\varphi (\Omega_0 - \omega) dt$ , by introducing small quasi-Cartesian  $x$  and  $y$  variables:

$$x^{(r)} = e^{\mu_1} R_0 + x, \quad dx^{(\varphi)} = e^\varphi (\Omega_0 - \omega) dt + dy. \quad (38)$$

We assume the local force drawing the displaced particle back to its unperturbed location,  $-Kx$ ,  $-Ky$ , where  $K$  is the some positive constant. The linearized equations are written by

$$\ddot{x} - 2\Omega_{\tilde{\tau}} \dot{y} - \tilde{\chi}^2 x = -Kx, \quad \ddot{y} + \kappa_{\tilde{\tau}} \dot{x} = -Ky. \quad (39)$$

where

$$\Omega_{\tilde{\tau}} = v_{(\varphi)} \tilde{\nabla}^{(r)} \ln e^\psi - \frac{1}{2} v_\omega \tilde{\nabla}^{(r)} \ln \omega, \quad \tilde{\chi}^2 = -2v_\omega \Omega_{\tilde{\tau}} \tilde{\nabla}^{(r)} \ln \omega \quad \text{and} \quad \kappa_{\tilde{\tau}} = 2v_{(\varphi)} \tilde{\nabla}^{(r)} \ln e^\psi \quad (40)$$

and the dots denote the time derivatives,  $\ddot{x} = \partial^2 x / \partial \tilde{\tau}^2$ .

The  $x$  and  $y$  displacements have solutions to the above equations varying as  $e^{i\tilde{\Gamma}\tilde{\tau}}$ , with

$$\check{\Gamma}^4 - \check{\Gamma}^2(\tilde{\kappa}^2 - \tilde{\chi}^2) - K\tilde{\kappa}^2 = 0, \quad (41)$$

where  $\check{\Gamma}^2 = \tilde{\Gamma}^2 - K$  and  $\tilde{\kappa}^2 = 2\Omega_{\tilde{\tau}} \kappa_{\tilde{\tau}}$ . The above dispersion relation leads the following expression of the maximum growth rate,

$$\tilde{\Gamma}_{max}^2 = -\frac{\tilde{\chi}^4}{4\tilde{\kappa}^2}. \quad (42)$$

Far away from a black hole the functions,  $\tilde{\chi}^2$  and  $\tilde{\kappa}^2$ , are approximately represented by

$$\tilde{\chi}^2 \sim -\frac{d\Omega^2}{d \ln r}, \quad \tilde{\kappa}^2 \sim \frac{2\Omega}{r} \frac{d(r^2\Omega)}{dr}. \quad (43)$$

Then the maximum growth rate approaches to the local Oort  $A$ -value:

$$|\tilde{\Gamma}_{max}| \sim -\frac{1}{2} \frac{d\Omega}{d \ln r}. \quad (44)$$

Thus the dispersion relation (41) is the general relativistic version analogous to the dynamical shear instability in which the maximum growth rate is the local Oort  $A$ -value.

We show the variations of the maximum growth rate  $\bar{\Gamma}_{max}^2(r)$  and the related functions  $\bar{\kappa}^2$  and  $\bar{\chi}^2$  for  $a = M, 0$  in Fig.7. Here we represent the dimensionless variables defined by  $\bar{\Gamma} = \tilde{\Gamma}/\tilde{\Omega}$ ,  $\bar{\chi} = \chi/\tilde{\Omega}$ ,  $\bar{\kappa} = \tilde{\kappa}/\tilde{\Omega}$ .

It is a distinctive feature in DSI that at the inner limit,  $r \rightarrow r_{ms}$ , the maximum growth rate  $|\bar{\Gamma}_{max}(r)|$  for  $a = M$  reaches to  $\infty$ . Here the function corresponding to the epicyclic frequency  $\tilde{\kappa}$  approaches to infinitesimal,  $\tilde{\kappa} \rightarrow \sqrt{2}(r - r_{ms}) \rightarrow 0$ , when  $r \rightarrow r_{ms}$  while the function representing the shear  $\tilde{\chi}^2$  is finite at the inner limit,  $\tilde{\chi}^2 \rightarrow 3$ . The growth rate thus becomes  $|\tilde{\Gamma}_{max}| = 3/(2\sqrt{2}(r/r_{ms} - 1)) \rightarrow \infty$  for  $r \rightarrow r_{ms}$ . The maximum growth rate in DSI is remarkably different from that in MRI when  $a = M$  and  $r = r_{ms}$ .

This distinctive difference in  $\bar{\Gamma}_{max}$  between MRI and DSI is understood with the dispersion relations, (41) and (26). The shear term containing the differential angular velocity  $\nabla \ln \Omega$ , i.e.,  $\tilde{\chi}^2$ , is inserted in the parenthesis at the second term on the left hand of (41) while it is in the third term in (26). It leads the different expressions in the maximum growth rate between (32) and (42). for  $r \rightarrow r_{ms}$ , the maximum growth rate  $\bar{\Gamma}_{max}$  expressed by (32) becomes finite when  $\bar{\kappa}^2 \rightarrow 0$ .

In DSI the term  $\tilde{\chi}^2$  is produced in the perturbation of “gravitational force” in the radial direction (36). In MRI the term containing  $\nabla \ln \Omega$  appears in the dynamics in the azimuthal direction (20) through the perturbation of the azimuthal component of magnetic field  $\delta B^{\hat{\phi}}$ . In the Newtonian limit, the angular velocity with the power law dependence of radius,  $\Omega \propto r^{-3/2}$ , reduces the differences of the coefficients in the dispersion relation between (26) and (41) to disappear, as follows ;  $\kappa^2 \rightarrow \Omega^2$ ,  $\kappa^2 + \chi^2 \rightarrow 4\Omega^2$ , in (26) and  $\tilde{\kappa}^2 - \tilde{\chi}^2 \rightarrow \Omega^2$ ,  $\tilde{\kappa}^2 \rightarrow 4\Omega^2$  in (41). However in rotating spacetime geometry the differential rotation of the geometry,  $v_{\omega} \nabla \ln \omega$ , becomes a main term in these functions. It is concluded that there exist remarkable differences in the dispersion relation between MRI and DSI.

The behavior of maximum growth rate  $\tilde{\Gamma}_{max}(r)$  in DSI is fairly different from that given by Gammie (2004). He showed that the maximum growth rate normalized by Newtonian Oort  $A$ -value,  $|\Gamma_{max}|/[(3/4)(Mr^{-3})^{-1/2}]$ , is restricted between 1 and 4/3 for all radii and for all  $a$ . His method deriving the dispersion relation is different in some aspects from ours. He had analyzed the dynamics of perturbations in the Boyer-Lindquist coordinate frames (BLCF) in which the observer measures the motion of a particle with clock and rule at the distance far from a hole. We have also re-derived the dispersion relation of DSI in BLRF with the similar forms as in LNRF, which is shown in Appendix B. Then the function corresponding to the epicyclic frequency  $\tilde{\kappa}$  reaches to  $\infty$  when  $r \rightarrow r_{ms}$  and  $a \rightarrow 1$ . Thus

the maximum growth rate at  $r \rightarrow r_{ms}$  becomes infinitesimal,  $\Gamma_{max} \rightarrow 0$ , which is contrary to the above result in LNRF.

When  $a = M$ , the asymptotic behavior of  $\kappa_{\tilde{r}}$  at  $r \rightarrow r_{ms}$  is extremely different between BLCF and LNRF. This difference is caused by the expression of the circular velocity measured in each of frame. In BLCF the coefficient  $\kappa_{\tilde{r}}$  in (B9) is described with the velocities,  $v_\Omega$  and  $v_\omega$  which become infinity at  $r \rightarrow r_{ms}$ , while in LNRF  $\kappa_{\tilde{r}}$  in (40) is expressed with  $v_{(\varphi)}$  which is limited within 1/2 for  $r \leq r_{ms}$ . The function  $\kappa_{\tilde{r}}$  in (40) (LNRF) reduces to zero for  $r \rightarrow r_{ms}$  since the covariant derivative  $\tilde{\nabla}^{(r)} \ln e^\psi$  becomes infinitesimal at  $r \rightarrow r_{ms}$ . The dynamics in the azimuthal direction is exerted by the "Coriolis force"  $\tilde{\kappa}_{\tilde{r}} \dot{x}$ . In BLCF the rapidly rotating particle perturbed by  $\dot{x}$  is extremely accelerated in the azimuthal direction. The dynamics of perturbed motion at  $r \sim r_{ms}$  is very different between BLCF and LNRF.

The perturbed quantities in LNRF are not same as in BLCF. The perturbed velocity in the radial direction in LNRF,  $\dot{x}$ , is divided into two components, radial and azimuthal ones, in BLCF. Then its azimuthal component becomes not always a first order of small quantity in BLCF, and vice versa. Thus the dispersion relation becomes definitely different between LNRF and BLCF.

The LNRF is suitable for the analysis of perturbations around a rotating black hole since the dragging of inertial frames becomes so severe in BLCF that the  $t$  coordinate basis vector  $(\partial/\partial t)$  goes spacelike at the static limit  $r_0$ . Thus it is concluded that the both types of instabilities, DSI and MRI, are remarkably enhanced in the vicinity of a rapidly rotating black hole, though their growth rates are not same.

A summary of the results is as follows. The dispersion relation in MRI is represented in general relativistic forms. The growth rate at  $r \approx r_{ms}$  is realized for  $a = M$  by the rotation of spacetime geometry. The maximum growth rate  $|\bar{\Gamma}_{max}|$  at  $r = r_{ms}$  for  $a = M$  is about one-order of magnitude larger than that for  $a = 0$ . When the magnetic field is so intensive that  $v_A \geq 0.1c$ , the over stability mode becomes remarkable and its growth rate increases according to the strength of magnetic field. The shear instability, MRI or DSI, is largely enhanced by the rapidly rotating black hole though the value of maximum growth rate in DSI is fairly different from that in MRI. The dispersion relation at  $r \approx r_{ms}$  is suitably evaluated in LNRF. In the static geometry the growth rates in MRI and DSI remain almost in similar variation as in Newtonian case.

We are grateful to Professors T. Ishizuka and T. Yoshida for useful discussion and advice on the magnetorotational instability in curved spacetime.

### A. Coefficients of the Affine Connection in the Orbiting Frame

The rotation one-forms  $\omega_\nu^\mu$  are derived from the one-forms  $\vec{\omega}^\lambda$  shown in (5) (Punsly 2001; Misner, Thorn & Wheeler 1970). From the one-form  $\vec{\omega}^\nu = \beta_\lambda^\nu \mathbf{d}x^\lambda$ , we compute the exterior derivative

$$\mathbf{d}\vec{\omega}^\nu = \frac{\partial \beta_\lambda^\nu}{\partial x^\mu} \mathbf{d}x^\mu \wedge \mathbf{d}x^\lambda = -\omega_\mu^\nu \wedge \vec{\omega}^\mu. \quad (\text{A1})$$

The coefficients of Affine connection  $\Gamma_{\mu\lambda}^\nu$  are read off the representation  $\omega_\mu^\nu = \Gamma_{\mu\lambda}^\nu \vec{\omega}^\lambda$ .

Their explicit expressions are as follows:

$$\begin{aligned} \Gamma_{\hat{r}\hat{t}}^{\hat{t}} &= e^b \nabla^{\hat{r}} \ln \hat{\alpha} - v_{(\varphi)} v_\Omega \gamma^2 \nabla^{\hat{r}} \ln(\gamma e^\psi v_{(\varphi)}), \\ \Gamma_{\hat{r}\hat{\varphi}}^{\hat{t}} &= \frac{1}{2} \gamma^2 (v_\Omega \nabla^{\hat{r}} \ln \Omega - e^b v_{(\varphi)} \nabla^{\hat{r}} \ln(\gamma e^\psi v_{(\varphi)} / \hat{\alpha})), \\ \Gamma_{\hat{\theta}\hat{t}}^{\hat{t}} &= e^b \nabla^{\hat{\theta}} \ln \hat{\alpha} - v_{(\varphi)} v_\Omega \gamma^2 \nabla^{\hat{\theta}} \ln(\gamma e^\psi v_{(\varphi)}), \\ \Gamma_{\hat{\theta}\hat{\varphi}}^{\hat{t}} &= \frac{1}{2} v_\Omega \gamma^2 \nabla^{\hat{\theta}} \ln \Omega - e^b v_{(\varphi)} \nabla^{\hat{\theta}} \ln(\gamma e^\psi v_{(\varphi)} / \hat{\alpha}), \\ \Gamma_{\hat{\varphi}\hat{r}}^{\hat{t}} &= \Gamma_{\hat{\varphi}\hat{t}}^{\hat{r}} = \frac{1}{2} v_\Omega \gamma^2 \nabla^{\hat{r}} \ln \Omega, \\ \Gamma_{\hat{\varphi}\hat{\theta}}^{\hat{t}} &= \Gamma_{\hat{\varphi}\hat{t}}^{\hat{\theta}} = \frac{1}{2} v_\Omega \gamma^2 \nabla^{\hat{\theta}} \ln \Omega, \\ \Gamma_{\hat{\theta}\hat{r}}^{\hat{r}} &= \nabla^{\hat{\theta}} \ln e^{\mu_1}, \quad \Gamma_{\hat{\theta}\hat{\theta}}^{\hat{r}} = -\nabla^{\hat{r}} \ln e^{\mu_2}, \\ \Gamma_{\hat{\varphi}\hat{\varphi}}^{\hat{r}} &= -\nabla^{\hat{r}} \ln(\gamma e^\psi) + v_{(\varphi)} v_\Omega \gamma^2 \nabla^{\hat{r}} \ln \Omega, \\ \Gamma_{\hat{\varphi}\hat{\varphi}}^{\hat{\theta}} &= -\nabla^{\hat{\theta}} \ln(\gamma e^\psi) + v_{(\varphi)} v_\Omega \gamma^2 \nabla^{\hat{\theta}} \ln \Omega. \end{aligned}$$

### B. The Dynamical Shear Instability in the Boyer-Lindquist Coordinate Frame

The equation of motion of a particle is described in the Boyer-Lindquist coordinate frame (BLCF) by,

$$\frac{d^2 x^\lambda}{d\tau^2} + \Gamma_{\mu\nu}^\lambda \frac{dx^\mu}{d\tau} \frac{dx^\nu}{d\tau} = 0, \quad (\text{B1})$$

where  $\Gamma_{\mu\nu}^\lambda$  are the coefficients of Affine connection in BLCF. When the motion is restricted in the equatorial plane, these equations are represented by using the expressions of coordinates,  $x^{(r)}$ ,  $x^{(\varphi)}$ , and the covariant derivative,  $\tilde{\nabla}^{(r)}$ , in L NRF as

$$\begin{aligned} \frac{d^2 x^{(r)}}{\alpha^2 dt^2} + \tilde{\nabla}^{(r)} \ln \alpha + v_\omega \frac{dx^{(\varphi)}}{\alpha dt} \tilde{\nabla}^{(r)} \ln(\omega e^\psi) - \left( \frac{dx^{(\varphi)}}{\alpha dt} \right)^2 \tilde{\nabla}^{(r)} \ln e^\psi &= 0, \\ \frac{d^2 x^{(\varphi)}}{\alpha^2 dt^2} + \left\{ v_\Omega \left[ 2\tilde{\nabla}^{(r)} \ln e^\varphi + v_\omega^2 \tilde{\nabla}^{(r)} \ln \omega \right] \right. & \quad (\text{B2}) \end{aligned}$$

$$- v_\omega \left[ 2\tilde{\nabla}^{(r)} \ln v_\omega - (1 - v_\omega^2)\tilde{\nabla}^{(r)} \ln \omega \right] \frac{dx^{(r)}}{\alpha dt} = 0. \quad (\text{B3})$$

Let's consider the situation of perturbations that the particle is allowed to make small excursions from a circular orbit,  $r = R_0$ ,  $\varphi = \Omega_0 t$ , by introducing small quasi-Cartesian  $x$  and  $y$  variables:

$$r = R_0 + x e^{-\mu_1}, \quad \varphi = \Omega_0 t + y e^{-\psi}. \quad (\text{B4})$$

The linearized equations are then written by

$$\begin{aligned} \ddot{x} &- 2v_{(\varphi)} \dot{y} \tilde{\nabla}^{(r)} \ln e^\psi + \dot{y} v_\omega \tilde{\nabla}^{(r)} \ln(\omega e^\psi) \\ &+ e^{2(\psi-\nu)} \tilde{\nabla}^{(r)} \Omega^2 \left[ \nabla^{(r)} \ln e^\psi - \frac{\omega}{2\Omega} \tilde{\nabla}^{(r)} \ln(\omega e^{3\psi}) \right] x = -Kx, \end{aligned} \quad (\text{B5})$$

$$\begin{aligned} \ddot{y} &+ \left\{ v_\Omega \left[ 2\tilde{\nabla}^{(r)} \ln e^\varphi + v_\omega^2 \tilde{\nabla}^{(r)} \ln \omega \right] \right. \\ &\left. - v_\omega \left[ 2\tilde{\nabla}^{(r)} \ln v_\omega - (1 - v_\omega^2)\tilde{\nabla}^{(r)} \ln \omega \right] \right\} \dot{x} = -Ky, \end{aligned} \quad (\text{B6})$$

We follow the convention of writing dots for time derivatives, e.g.,  $\ddot{x} = d^2x/(\alpha^2 dt^2) = d^2x/d\tilde{\tau}^2$ .

The  $x$  and  $y$  displacements have solutions to the above equations varying as  $e^{i\tilde{\Gamma}\tilde{\tau}}$ , with

$$\tilde{\Gamma}^4 - \tilde{\Gamma}^2(\tilde{\kappa}^2 - \tilde{\chi}^2 + 2K) + K(K - \tilde{\chi}^2) = 0, \quad (\text{B7})$$

where

$$\tilde{\chi}^2 = -e^{2(\psi-\nu)} \tilde{\nabla}^{(r)} \Omega^2 \left[ \tilde{\nabla}^{(r)} \ln e^\psi - \frac{\omega}{2\Omega} \tilde{\nabla}^{(r)} \ln(\omega e^{3\psi}) \right], \quad (\text{B8})$$

$$\begin{aligned} \tilde{\kappa}^2 &= 4v_\Omega v_{(\varphi)} \left\{ \left[ \tilde{\nabla}^{(r)} \ln e^\varphi + \frac{1}{2} v_\omega^2 \tilde{\nabla}^{(r)} \ln \omega \right] - \frac{\omega}{\Omega} \left[ \tilde{\nabla}^{(r)} \ln v_\omega - \frac{1}{2} (1 - v_\omega^2) \tilde{\nabla}^{(r)} \ln \omega \right] \right\} \\ &\times \left[ \tilde{\nabla}^{(r)} \ln e^\psi - \frac{\omega}{2(\Omega - \omega)} \tilde{\nabla}^{(r)} \ln(\omega e^\psi) \right]. \end{aligned} \quad (\text{B9})$$

The above dispersion relation gives the maximum growth rate,

$$\tilde{\Gamma}_{max}^2 = -\frac{\tilde{\chi}^4}{4\tilde{\kappa}^2}. \quad (\text{B10})$$

Far away from a black hole the functions,  $\tilde{\chi}^2$  and  $\tilde{\kappa}^2$ , are approximately represented by

$$\tilde{\chi}^2 \sim -\frac{d\Omega^2}{d \ln r}, \quad \tilde{\kappa}^2 \sim \frac{2\Omega}{r} \frac{d(r^2 \Omega)}{dr}. \quad (\text{B11})$$

The above maximum growth rate then has the local Oort  $A$ -value:

$$|\tilde{\Gamma}_{max}| \sim -\frac{1}{2} \frac{d\Omega}{d \ln r}. \quad (\text{B12})$$



We show in Fig.9 the maximum growth rate  $\bar{\Gamma}_{max}^2(r)$  and the related functions,  $\bar{\kappa}^2(r)$ ,  $\bar{\chi}^2(r)$  for  $a = M$ . Here we use the angular velocity of a circularly orbiting particle measured in LNRF,  $\tilde{\Omega} \equiv (\Omega - \omega)/\alpha$ , to define the dimensionless variables such as  $\bar{\Gamma} = \tilde{\Gamma}/\tilde{\Omega}$ ,  $\bar{\chi} = \tilde{\chi}/\tilde{\Omega}$  and  $\bar{\kappa} = \tilde{\kappa}/\tilde{\Omega}$ . The absolute value of the growth rate,  $|\bar{\Gamma}_{max}|$ , for  $a = M$  has an upper bound,  $|\bar{\Gamma}_{max}| \leq 1.5$ , which is a contrast to the maximum growth rate in LNRF. When  $a = 0$ , there is no large variation in  $\bar{\Gamma}_{max}^2(r)$  for the space,  $r \geq r_{ms}$ .

At the inner limit,  $r \rightarrow r_{ms}$ , the corresponding dimensionless functions for  $a = M$  become

$$\bar{\chi}^2 \rightarrow 3 \cdot 2^8, \quad \bar{\kappa}^2 \rightarrow \infty. \quad (\text{B13})$$

The infinity of  $\bar{\kappa}^2$  is brought about by  $v_\omega \rightarrow \infty$  when  $r \rightarrow r_{ms}$ . However the corresponding function  $\bar{\kappa}^2$  in the case of LNRF reduces to infinitesimal at  $r \rightarrow r_{ms}$ . While the growth rate expressed by (B10) reduces to infinitesimal at  $r \rightarrow r_{ms}$ , the growth rate expressed by (42) reaches to  $\infty$ . In the curved spacetime the dynamical shear instability in BLCF has the form unlike as in LNRF.

## REFERENCES

- Balbus, S. A., & Hawley, J.F. 1991, ApJ, 376, 214
- Balbus, S. A., & Hawley, J.F. 1992, ApJ, 392, 662
- Balbus, S. A., & Hawley, J.F. 1998, Rev. Mod. Phys., 70, 1
- Bardeen J. M., Press W. H., & Teukolsky S. A., 1972, ApJ, 178, 347
- Blandford, R.D., & Znajek, R.L. 1977, MNRAS, 179, 433
- Brandenburg, A., Nordlund, A., Stein, R. F., & Torkelsson, U. 1995, ApJ, 446, 741
- De Villers, J.P., Hawley, J.F., & Krolik, J.H. 2003, ApJ, 599, 1238
- Di Matteo T., Perna R., & Narayan R., 2002, ApJ, 579, 706
- Gammie, C. F., 2004, ApJ, 614, 309, Footnote 7 in Gammie, C. F., Popham, R. 1998, ApJ, 498, 313
- Balbus, S. A., & Hawley, J.F. 1991, ApJ, 376, 214
- Hawley, J. F., Gammie, C. F., & Balbus, S. A. 1995, ApJ, 440, 742

- Kawabata K. S., et al. 2003, ApJ, 593, L19
- Kohri K., & Mineshige S. 2002, ApJ, 577, 311
- Lipkin Y. M., et al., 2004, astro-ph/0312594
- Macdonald, D. A., & Thorne, Kip S. 1982, MNRAS, 198, 345
- MacFadyen, A.I., & Woosley, S.E., 1999, ApJ, 524, 262
- MacFadyen, A. I., Woosley, S. E., & Heger, A. 2001, ApJ, 550, 410
- Matheson T., et al., 2003, ApJ, 599, 394
- Matsumoto, R., & Tajima, T. 1995, ApJ, 445, 767
- Misner, C.W., Thorne, K.S., & Wheeler, J.A. 1970, Gravitation, W.H. Freeman and Company(San Francisco), 350
- Popham R., Woosley S.E., & Fryer, C., 1999, ApJ, 518, 356
- Punsly, B. 2001, Black Hole Gravitohydromagnetics, Springer(Berlin), 81
- Stone, J. M., Hawley, J. F., Gammie, C. F., & Balbus, S. B. 1996, ApJ, 463, 656
- Thorne, Kip S., & Macdonald, D. 1982, MNRAS, 198, 339
- Thorne, Kip S., Price, R. H., & Macdonald, D. A. 1986, Black Holes: The Membrane Paradigm, Yale University Press, 73
- Yokosawa, M., Uematsu, S., & Abe, J., 2004, MNRAS, submitted

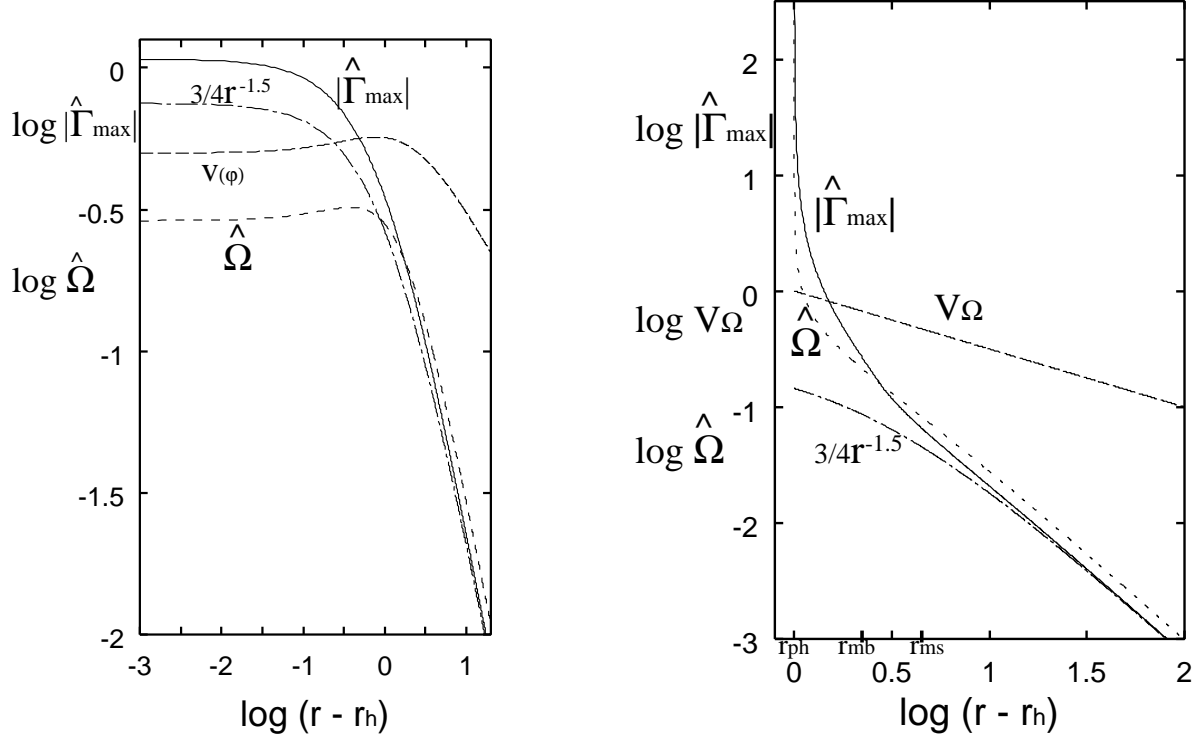


Fig. 1.— The distributions of the maximum proper growth rate  $|\hat{\Gamma}_{\max}(r)|$ , proper angular velocity  $\hat{\Omega}(r)$  and the function  $3/4r^{-3/2}$  on the distance from the event horizon. The left figure is shown in the case of the extreme Kerr metric and the right one is that of Schwarzschild metric. Other parameters are  $k^{\hat{r}} = 0$ ,  $N_{\hat{\theta}}^2 = 0.8\hat{\Omega}^2$ ,  $N_{\hat{r}}^2 = 0.01N_{\hat{\theta}}^2$ .

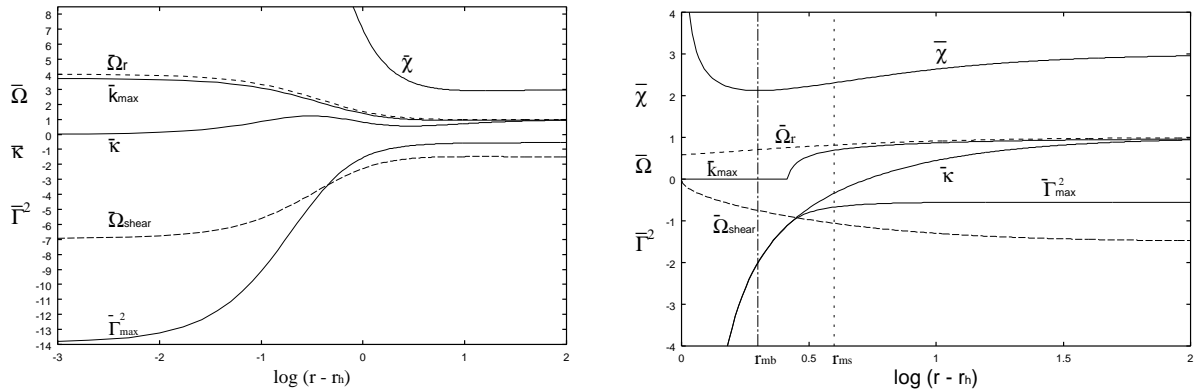


Fig. 2.— The distributions of the maximum relative growth rate  $\bar{\Gamma}_{\max}^2(r)$  and the related terms  $\bar{k}_{\max}(r)$ ,  $\bar{\chi}^2(r)$ ,  $\bar{\Omega}_{\hat{r}}(r)$  and  $\bar{\Omega}_{\text{shear}}(r)$  on the distance from the event horizon: The left figure shows the case of the extreme Kerr metric. The right figure shows the case of the Schwarzschild metric. Other parameters are same as in Fig.1.

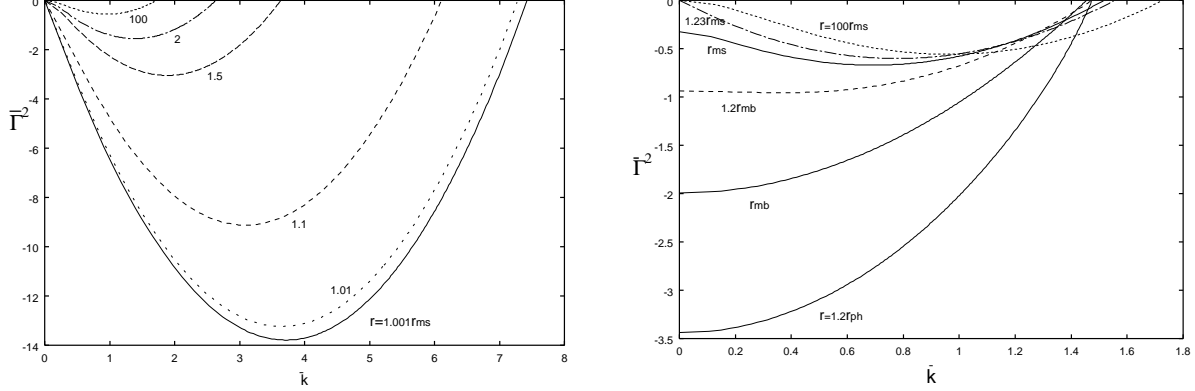


Fig. 3.— Dispersion relation: The Left figure shows the relative growth rates for the metric of an extreme Kerr. The squares of growth rate relative to the angular velocity  $\bar{\Gamma}^2 = (\hat{\Gamma}/\hat{\Omega})^2$ . are depicted. The wavenumber is normalized as  $\bar{k} = \mathbf{k} \cdot \mathbf{v}_A/\hat{\Omega}$ . The curves are correspond in order to  $r = 10^2, 2, 1.5, 1.1, 1.01, 1.001(r_{ms})$  from the top. The right figure shows the relative growth rates for the Schwarzschild metric. The curves are correspondent to  $r = 10^2 r_{ms}, 1.23 r_{ms}, 1 r_{ms}, 1.2 r_{mb}, 1.0 r_{mb}, 1.2 r_{ph}$ . Other parameters are same as in Fig. 1.

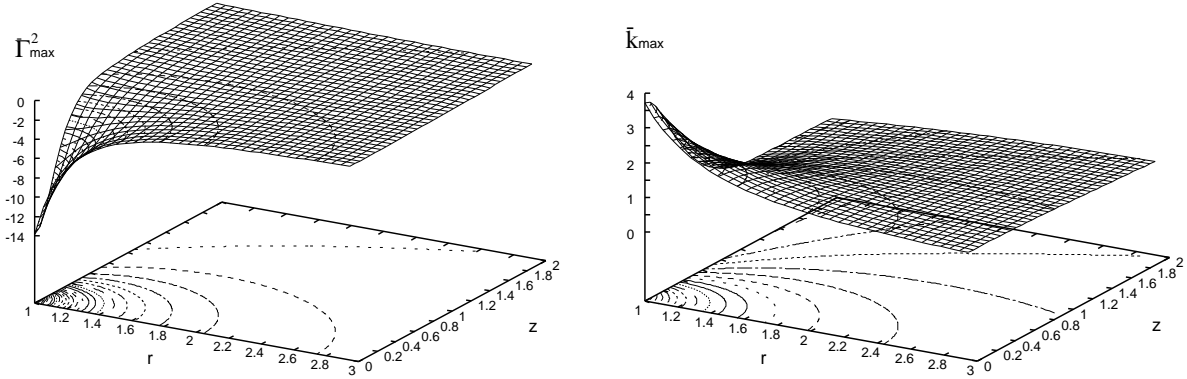


Fig. 4.— The left figure shows the distribution of the maximum relative growth rate  $\bar{\Gamma}_{max}^2(r, z)$  for  $a = M$ . The right figure shows the distribution of wave number  $\bar{k}_{max}(r, z)$  at the maximum growth rate. Other parameters are same as in Fig. 1.

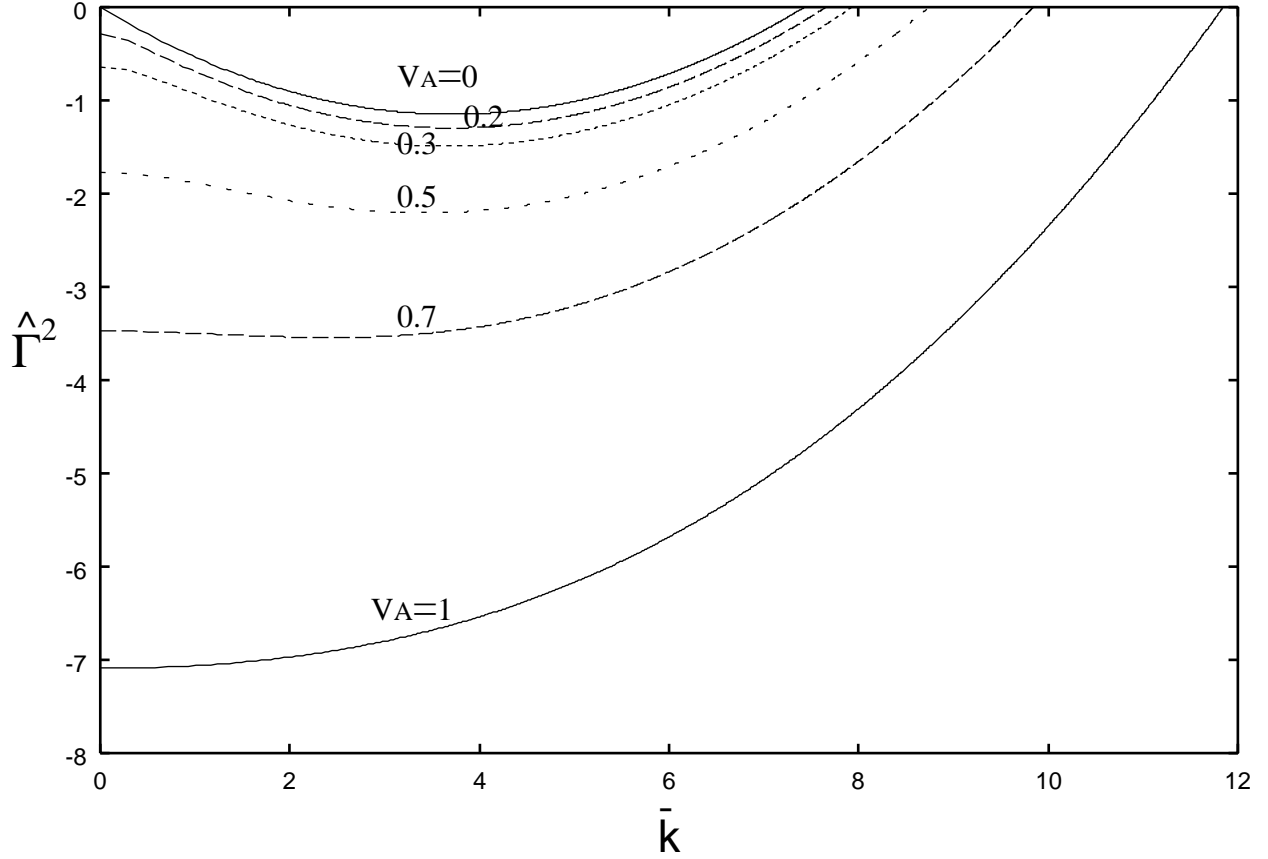


Fig. 5.— Dispersion relations with the term of magnetic induction due to the differential rotation of the orbiting frame. The proper growth rates  $\hat{\Gamma}^2$  are shown as the functions of the normalized wavenumber  $\bar{k} = \mathbf{k} \cdot \mathbf{v}_A / \hat{\Omega}$ . The curves are corresponding to the values of Alfvén velocity in unit of light velocity. The metric of spacetime is an extreme Kerr. The position is at  $r = 1.001r_{ms}$ . Other parameters are same as in Fig. 1.

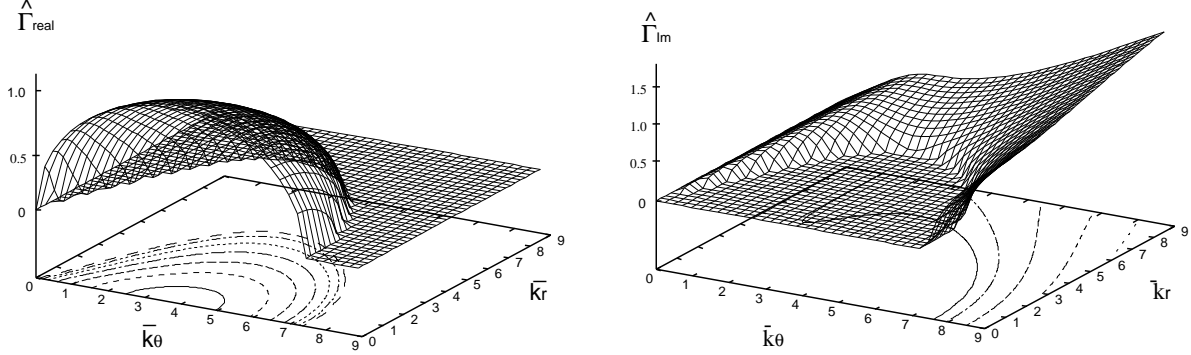


Fig. 6.— Three-dimensional plot of the unstable branch of the dispersion relation with  $v_A = 10^{-3}$ . Left figure: The real component of the growth rate  $\bar{\Gamma}_{real}(k_{\hat{\theta}}, k_{\hat{r}})$  is plotted in the  $\bar{k}_\theta (= k_{\hat{\theta}} v_A / \hat{\Omega}), \bar{k}_r (= k_{\hat{r}} v_A / \hat{\Omega})$  plane. The direction of magnetic field is fixed to be  $\mathbf{B} = B^{\hat{\theta}} \mathbf{n}_{\hat{\theta}}$ . The spacetime of the extreme Kerr is selected and the position is set to be  $r = 1.001 r_{ms}$ . Other parameters are same in Fig. 1. Right figure: Two-dimensional plot of the imaginary component of the growth rate  $\bar{\Gamma}_{Im}(k_{\hat{\theta}}, k_{\hat{r}})$ .

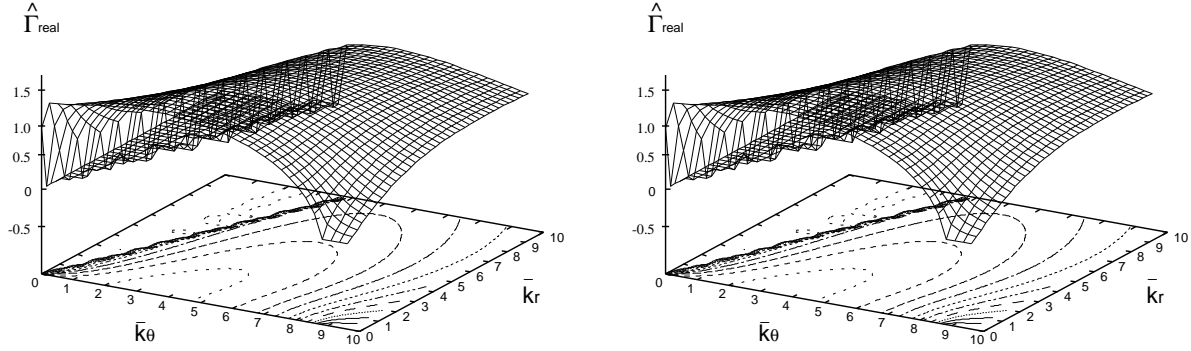


Fig. 7.— The left panel shows the three-dimensional plot of the unstable branch of the dispersion relation with  $v = 0.5c$ . The right panel shows the two-dimensional plot of the imaginary component of the growth rate  $\bar{\Gamma}_{Im}(k_{\hat{\theta}}, k_{\hat{r}})$ . Others are same in Fig. 6.

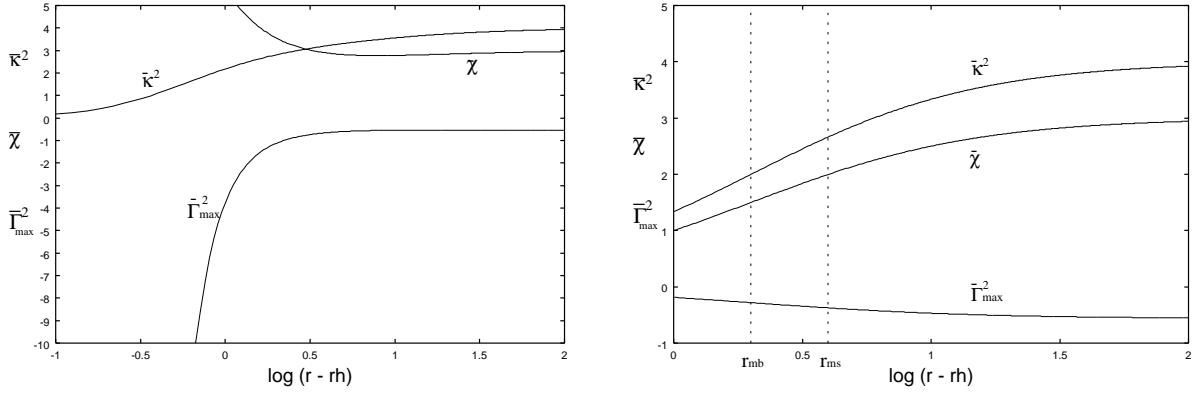


Fig. 8.— The distributions of the maximum growth rate  $\bar{\Gamma}_{max}(r)$  and the related terms  $\bar{\chi}^2(r), \bar{\kappa}^2(r)$  for the dynamical shear instability at the distance from the event horizon: The dispersion relation is driven in LNRF. The left figure is shown for  $a = M$  and the right one is for  $a = 0$ .

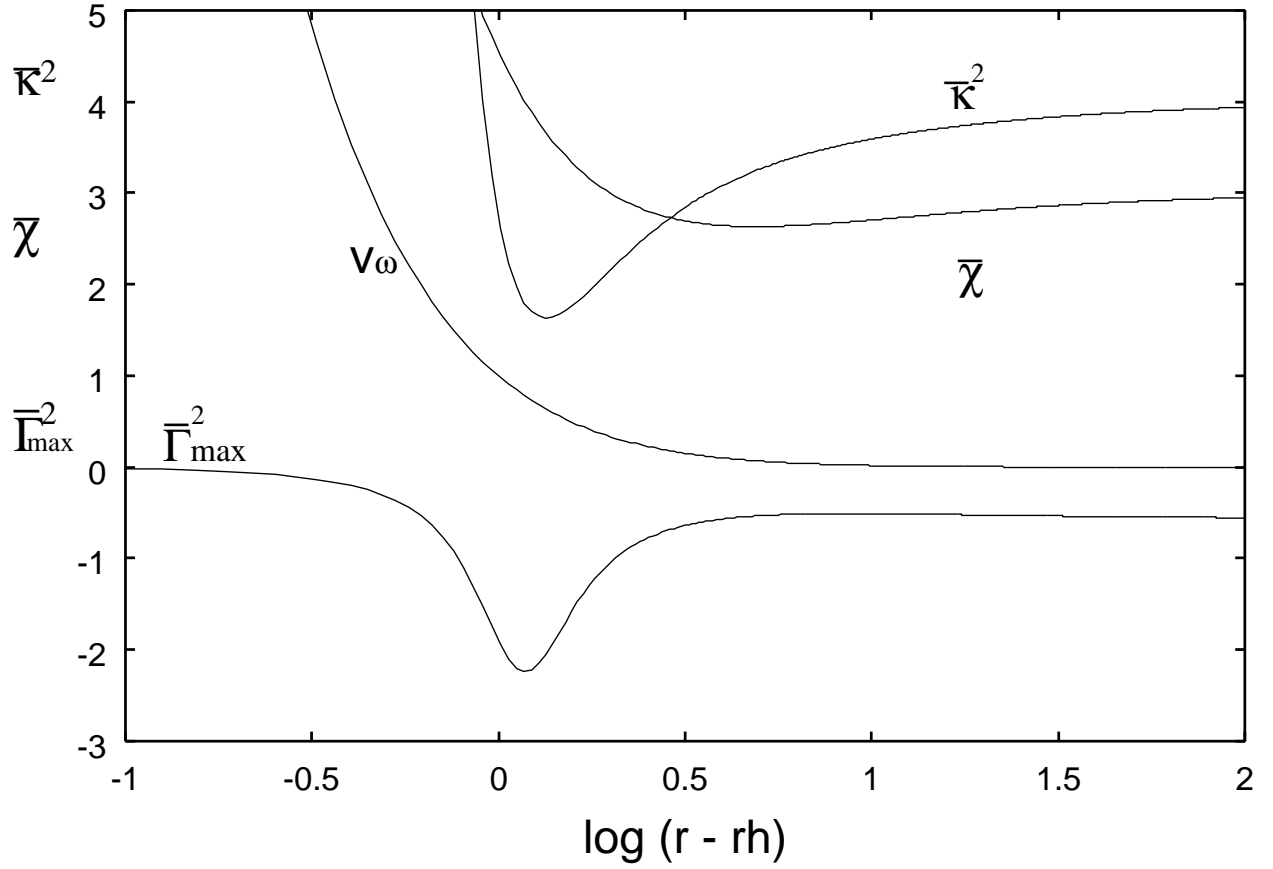


Fig. 9.— The distributions of the maximum growth rate  $\bar{\Gamma}_{max}(r)$  and the related functions  $\bar{\chi}^2(r)$ ,  $\bar{\kappa}^2(r)$ ,  $v_\omega(r)$  in the dynamical shear instability expressed in the Boyer-Lindquist coordinate frame. The metric of spacetime is the extreme Kerr.



